“Synthesis and Characterization of Niobium Aluminium Carbide”

A

Thesis

Submitted for the award of degree of

Masters of Science

By

Monika Gorsi
301404013

Under the guidance of

Dr. O. P. Pandey
Senior Professor and Dean (R & SP)

School of Physics and Materials science,

Thapar University, Patiala (Punjab)-147004

July 2016

CERTIFICATE

This is to certify that this dissertation entitled "Synthesis and Characterizations of Niobium Aluminium Carbide (Nb_2AlC) nano powder" is submitted by Monika Gorsi (Roll. No. 301404013) in the fulfilment of the requirement for the award of degree of Masters of Science in Physics from School of Physics and Materials Science, Thapar University, Patiala (Punjab), India. It is an exclusive record of candidate's own research under the supervision of Dr. O.P. Pandey. This dissertation in part or full has not been submitted in any other institution for the award of such kind of degree.

O.P. Pandey 13/7/2016

Dr. O.P. Pandey
(Supervisor)
Senior Professor and Dean R&SP
School of Physics and Materials Science
Thapar University, Patiala

Countersigned by:

Dr. M. K. Sharma
Professor and Head of Department
School of Physics and Materials Science,
Thapar University, Patiala

Dr. S. S. Bhatiya
Dean of Academic Affairs
Thapar University, Patiala

Acknowledgement

I am submitting my dissertation for the fulfilment of my 'M.Sc.' degree. This work would not have been accomplished without the support, help and guidance of a large number of people. I express my deep gratitude and respect to my supervisor **Dr. O. P. Pandey** (Senior Professor, School of Physics and Materials Science) for his keen interest, strong motivation and constant encouragement during the course of the work. I thank him for his great patience, constructive criticism and myriad useful suggestions apart from invaluable guidance to me.

I would also like to thank**Dr. Manoj Sharma** (Head of Department) and the entire esteem faculty members of School of Physics and Materials Science for their constructive suggestions at different stages of this work. My special thanks to **Dr. Kulveer Singh** and **Ms.Loveleen Kaur Brar** for their valuable suggestions.

I would like to thank to **Mr. Aayush Gupta**, **Ms. Mani Mahajan**, **Dr. Gurbinder Kaur**,**Mr. Gaurav Singla**, **Mr. Paramjyot Jha** for their patience, love, moral support and constant co-operation whenever I required.

The meaning of my life and work is incomplete without paying regards to my respected family whose blessings and continuous encouragement have shown me the path to achieve my goals.

And above all, I pay my regards to the Almighty for His blessings.

Monika

Monika Gorsi

Contents

List of Figures

List of Tables

Abstract

Due to the versatile properties like elastic stiffness, good thermal and electrical conductivity, resistance to chemical attack, and low thermal expansion coefficients, MAX phases have become a special group of compounds. They combine properties of both metals and ceramics so they find many applications in industries and aerospace. Among the large family of MAX phases, Nb_2AlC is potential candidate for high temperature applications. Therefore, in present study it was attempted to synthesise Nb_2AlC by ball milling using niobium pentaoxide (Nb_2O_5), activated charcoal as a carbon source, aluminium metal powder and magnesium as a reducing agent. The as-prepared samples were characterized and studied by X-ray powder diffraction, Field emission scanning electron microscopy and high resolution transmission electron microscopy at room temperature. Milling time and amount of reducing agent were optimized for the synthesise of Nb_2AlC. However, no signature of Nb_2AlC was observed in the synthesized samples and the resultant product is a nanocomposite comprising of NbC and Al_2O_3.

1 Introduction

Advanced materials are a necessary requirement for growth of modern society such as need of lightweight composites for faster vehicles, optical fibres finds uses in telecommunication world and silicon microchips for the information revolution. Many new materials are being synthesized every year. Among the four classes of materials (metals, non-metals, ceramics and composites), due to the ionic and covalent bonding of metallic and non-metallic element, ceramic materials have drawn great attention to be used in extreme environment of applications such as high temperature applications. These materials are thermally and electrically insulating, strong in compression, weak in shearing and tension, thermal shock resistant, brittle and hard. Ceramic materials can be classified into six categories such as; glasses, clays, refractories, abrasives, cements, and advanced or technical ceramics [1]. The advanced ceramics include silicon nitride, tungsten carbide etc. Silicon nitride combines mechanical, thermal and electrical properties which are basis of any advanced ceramic material. Due to its high strength and toughness it finds uses in automotive and bearing applications. Tungsten carbide due to its high hardness and wear resistance is used to make cutting tools and for abrasive water jet nozzles.

In recent years, carbides and nitrides have gained considerable attention as advanced materials due to their refractory nature, attractive chemical, physical properties and catalytic activities. Refractory carbides and nitrides are useful materials with wide range of technological applications and promising future [2]. Carbides/nitrides/borides are generally referred as MX phase, where M is a metal or non-metal and X is C/N/B.

1.1 MX Phase

MX phase or carbides/nitrides is a class of ceramic materials with exceptional profile of high melting temperatures, mechanical, physical, chemical and even biological properties. In a short span of time, they have emerged as useful industrial materials and have numerous applications such as cutting and grinding machinery, bearings, textile-machinery components and many others [3]. One of the major problem with these materials is hydrolysis at their surface, when stored under humid atmosphere. Due to combined action of humidity and oxygen cause changes on the surface ceramic layer [4]. They are highly brittle due to their low ductility which results low impact resistance of MX phases. Shear and tensile strengths are about 15 times less than that of the metals. They are difficult to design because of their high melting points and hardness.

In search of advanced ceramic materials, which play crucial role in future lightweight components in different fields like automobile and aerospace industries, researchers tried to develop a new group of materials, which combines the best properties. Metallo-Ceramics or MAX compounds, here 'M' stands for an early transition metal (Sc, Hf, Ta, Ti, V, Cr, Nb and Mo), 'A' stands for a group 'A' element (Cd, Ga, Ge, Pb, P, S, As, Al, Si, Sn, In etc.) and 'X' stands for carbon or nitrogen or boron, combine the properties of metals and ceramics, offering high potential, to be used in various engineering applications [5]. It is a class of ternary materials that provides a combination of ionic, covalent and metallic bonds. When MX monolayers are intertwined with monoatomic A layers, MAX phases are formed.

1.2 MAX Phase

In the series of advanced materials, a new name was added when 100 new carbides and nitrides were discovered by Nowotny's group. The discovery of bulk Ti_3SiC revolutionized the era which was reported to have excellent properties of metals as well as ceramics [5]. Some of the similarities between MAX and MX phase are:

(1) The M-M distance for MAX and MX phases is almost same.
(2) MX and MAX both are conducting in nature with conductivity equivalent to metals.
(3) The mechanical properties of MAX phases are same as their MX counterparts [6].

Unlike MX phases which are the hardest materials known, brittle, non-machinable, susceptible to thermal shocks, MAX phase are ductile highly machinable, thermal and resistant to chemical attack. This stark difference is due to the presence of numerous mobile dislocations at room temperature [7]. Due to these numerous properties, they have wide applications like heating elements, high-temperature foil bearings etc.

They have also attracted the attention of nuclear industries, oxidation barrier coating for the fuel cladding systems in the light water reactors and core components for advanced reactor concepts including the gas fast reactors. There are some of the MAX phases, specifically Ti_3AlC_2 and Ti_3SiC_2, are quite resistant to radiation damage, so they can be used in nuclear industries [8].

1.2.1 MAX: Crystal Structure

When a transition metal belonging to a A-group element (specifically from the group 13-16) are doped with carbon or nitrogen and are referred as metallo-ceramics or MAX phase, whose general formula is $M_{n+1}AX_n$. According to the value of n in family formula $M_{n+1}AX_n$ they are

divided into six groups: M_2AX (n=1), M_3AX_2 (n=2), M_4AX_3 (n=3), M_5AX_4 (n=4), M_6AX_5 (n=5) and M_7AX_6 (n=6). The different MAX stoichiometries are often referred to as 211 phase (corresponding to n =1), 312 phase (corresponding to n = 2), and 413 phase (corresponding to n = 3). Various possible elements for the formation MAX phases are highlighted in figure 1.1.

MAX phase is a subgroup of the much larger class of "layered ternary ceramics". The term "layered ternary ceramics" is commonly used for all the ceramics that have exactly three elements along with a layered structure. The crystal structure of MAX phase is a hexagonal type [9], where MX layers are twinned with respect to each other and separated by A layer which acts as mirror plane. MAX phases are interstitial compounds, where the interstitial sites between 'M' atoms are filled with 'A' and 'X' atoms. The stacking sequence is such that for M_2AX_3, every 2 'M' layers are separated by 1 'A' layer and similarly for M_3AX_2, every 3'M' layers are separated by 1 'A' layer and 'X' occupying the octahedral site as shown in figure 1.2. MAX phase structures are anisotropic in nature. With the increasing value of n, the structure becomes more complex and as a result thermodynamic stability decreases. The varying value of n, in $M_{n+1}AX_n$ formula gives rise to the crystal structure with increasing c/a parameter.

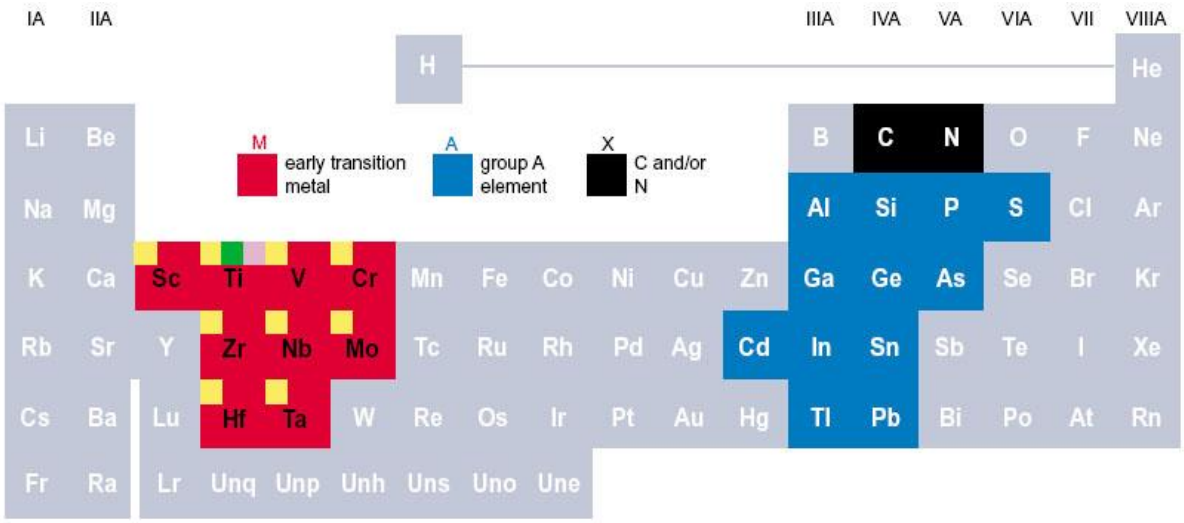

Figure 1.1: Shows the list of elements in periodic table that form MAX phase [11].

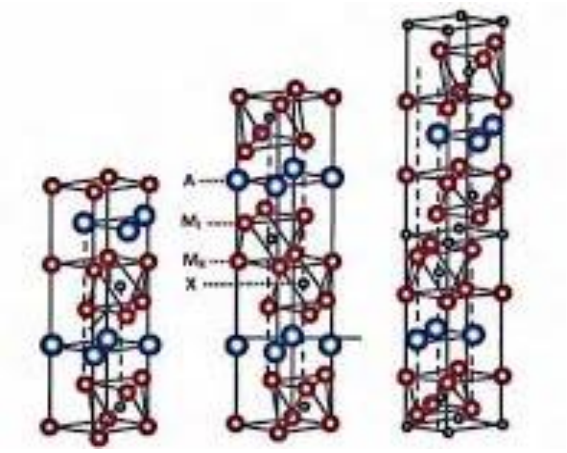

Figure 1.2: Shows the unit cells of 211, 312 and 413 MAX phase [11].

Apart from the phases discussed above (211, 312, 413, 514, 615 and 716), '523' and '725' phases also exist, which are termed as hybrid phases or intergrown structures. The structure for '523' phases can be understood as an amalgam of half unit cell of '312' and the other half corresponding to half-unit cell of '211'. Similarly, the phase '725' is a combination of '312' and '413' phases [10].

1.2.2 Bonding in MAX phase

The nature of bonding between M and A is metallic while bonding between M and X is covalent. These weak M-A bonding results in easy basal plane slip and low shear deformation resistance. Also the metallic M-A bonding and covalent M-X bonding result in exclusive blend of properties of both metals and ceramics [11]. Bonding in MAX phase are a combination of ionic, metallic and covalent bonds. The following are some noteworthy important points about bonding in MAX compounds;

- The p levels of X element and d levels of M elements strongly overlap each other resulting in strong covalent bonds [12].
- There is overlapping of p orbital of A atom and d orbital of M atom.
- The density of states at the Fermi level is substantial and consistent with high thermal and electrical conductivities.
- The d orbitals of M atom overlap with themselves and influence the density of states at Fermi level [13].

1.3 Properties of MAX Phases

MAX phases are thermodynamically stable at high temperatures, machinable, oxidation resistant. In addition to these they are shock resistant and damage tolerant, these properties are a result of mobile dislocations. The delaminations are stopped by kink bands, preventing them from further growth and making them damage tolerant. They were commercialized to make gas burner nozzles and heating elements in 2001 [14]. MAX phase based foil bearings are successfully developed which having low friction and wear upto 823 K. For example, Ta_2AlC/Ag. Since Ti_2AlC has a better oxidation and wear resistance and it is being used as a replacement for graphite at high temperatures. All the applications of MAX phases are only at macroscopic scale; their nanolaminated structure is not yet utilized for any powerful application. They are elastically quite stiff and have their densities comparable to Ti with Debye temperatures of 700 K [15-17]. The anisotropy is quite visible in all the properties of MAX phase [11]. The MAX phase is layered structure that shows conductivity anisotropy, the conductivity along the crystalline layers can be large as compared to the conductivity across the layers [18]. Due to anisotropy in chemical bonding and nanolaminated structure, it is assumed that the MAX phases possesse anisotropic compressibility. The compressibility of Ti_2AlC, V_2AlC and Ti_3SiC_2 are large along the c-axis than along a-axis. While opposite behaviour is observed for Cr_2AlC and Nb_2AlC [19]. However, Ta_2AlC has the same compressibility along both the axis [20]. Some of the properties, which define why MAX phases are the most interesting class of materials are as follows:

- Their electrical and thermal conductivities are excellent. For example, in comparison to its MX counterpart Ti_3SiC_2 have the electrical and thermal conductivity double to that of Ti metal.
- Vickers hardness for these materials lies in the range of 2-5 GPa, making them relatively soft as compared to other carbides and nitrides [21].
- These solids are exceptionally thermal shock resistant and damage tolerant.
- They are the only solids that exhibit fully reversible dislocation-based deformations [22].
- MAX phases are elastically stiff (at 320 GPa), Ti_3SiC_2 have same density as that of Ti metal with value 4.5 g/cm^3 but it is 3 times more stiffer than Ti metal. [21].
- They retain many of their properties and are thermally stable to very high temperatures (>1700 °C).

- Among the class of polycrystalline solids, MAX phases are the only solids in which deformation occur by kink and shear band formation.

1.3.1 Elastic Properties

MAX phase are elastically quite stiff. Some of MAX compounds have very low densities as 4−5 g/cm^3 but their specific stiffness can be higher. For example, specific stiffness of Ti_3SiC_2 is comparable to Si_3N_4. MAX phase with light A element are more stiff than those containing heavy A element like Pb, Sn and In [11]. Poisson's ratio gives the information about the overall bonding characteristics of the material and for all the MAX phases its value is 0.2 (approx.). Cr_2AlN has the largest Poisson's ratio, reflecting its metallic character and among the weakly coupled compounds. Most of the M_2AlX compounds exhibit a mixture of covalent-ionic-metallic bonding. Ta_2AlX, Cr_2AlC and Mo_2AlC have the highest shear, bulk and young's moduli. They are quite stiff and at room temperature, their Young's and shear moduli lie in 178−362 GPa and 80−142 GPa ranges, respectively. Since Ta_2AlN and Cr_2AlN have better ductile characteristics, so they can be used for structural applications [23]. All the MAX phases undergo brittle to ductile transition at high temperatures but this transition temperature varies from phase to phase. For example, many Al containing MAX phase has this value of transition temperature lying between 1000 °C to 1100 °C [11].

1.3.2 Physical Properties

All the MAX phases are good conductors of electricity. At room temperature their resistivities lie in precise range of 0.2−0.7 μΩ-m [18] and analogous to metals, their resistivity keeps increasing with increasing temperature. They are compensated conductors with equal concentration of electrons and holes. Delocalized electrons dominate and govern the optical properties of MAX phase. Magnetically, they are Pauli paramagnets whose susceptibility is determined by delocalized electrons. Like their MX counterparts, they conduct heat. At room temperature, their thermal conductivities fall in range 12−60 W/(m-K). The coefficient of thermal expansion for them, falls in the range of 5−10 μK^{-1}. The thermal expansion coefficient of Cr_2AlC is higher than most of the MAX phase compounds which proves its excellent ability as a protective coating for metals which acts as a barrier to oxidation and corrosion attack. They do not melt easily at significant high temperature, MAX phases undergoes decomposition to A-rich liquid. Ti_3SiC_2 is quite refractory with the decomposition temperature of 2300 °C [24].

1.3.3 Mechanical properties

In MAX phase compounds, basal plane dislocations are responsible for how they respond to applied stress. MAX compounds have only two slip systems operative. Thus they lie in a situation in which they are pseudoductile. This dearth of slip system results in a non-uniform stress distribution. The dislocations multiply and glide along basal planes, arrange either in arrays or walls. The interaction of dislocations pileups and grain boundaries is key to unique mechanical response of the MAX phases, from fracture toughness, to creep to tensile properties. Among all the M_2AlX phases, Mo_2AlN is the only mechanically unstable structure [25]. The phases with highest machinability index are W_2SnC, Mo_2PbC and Cr_2PbC. Here in MAX compounds, the phases with high sheerability have high machinability, example is W_2SnC has smallest value for sheerability and has the largest machinability index [23].

1.3.4 Electronic properties

The d-orbital of M atoms influences the electronic properties of MAX phases and these properties in turn are comparable to the transition metals. The resistivity of materials Ti_2AlC, Cr_2AlC, Nb_2AlC and V_2AlC drops linearly with decreasing temperature and this metal like behaviour of M/AX phase results from the high density of states at the Fermi level of these compounds. The total density of Al containing MAX carbide at Fermi level is a finite value which indicates that all Al containing compounds are conducting in nature. The total density of states at Fermi level is heavily affected by valence electron concentration (VEC) and d-electron shell number of M atoms. So, overall total density of states at Fermi level increases with increasing n and VEC and it decreases for phases M_3AlC_2 and M_4AlC_3, with increasing d-electron shell number [26].

1.3.5 Oxidation resistance

Oxidation behaviour of MAX phase is important property for ceramic applications at high temperature. The system of these ceramics: Titanium-Aluminium-Carbon, Titanium-Silicon(Aluminium)-Carbon and Chromium-Aluminium-Carbon show excellent oxidation as compared to other MAX compounds. The reason for such excellent behaviour lies in the fact that, it forms a protective Al_2O_3 layer. Extremely oxidation-resistant MAX phase is Ti_2AlC. Since Ti_2AlC has the capability to forms a stable and protective Al_2O_3 layer on its surface. This Al_2O_3 layer can bear thermal cycling up to 1,350 °C for 10,000 cycles without getting damaged [6].

1.3.6 Superconductivity

More than 70 MAX phases has been synthesised till now, bulk superconductivity is discovered for eight systems, Mo_2GaC [27], Nb_2SC [28], Nb_2SnC [29], Nb_2AsC [30], Ti_2InN [31] and Nb_2InC [32]. Since the mechanical properties of superconducting materials are of great importance. Among all the superconducting MAX phases Mo_2GaC has the largest bulk modulus and Ti_2InN has the smallest bulk modulus with 249 GPa and 125 GPa respectively. They are anisotropic and some of them are ductile (Mo_2GaC and Nb_2InC) and some are brittle (Nb_2SnC and Ti_2InC). The elastic parameters of these materials are higher than that of layered FeAs superconductors, and comparable to other superconductors like Yttrium barium copper oxide (YBCO), MgB_2 [33].

1.4 Factors affecting the properties of MAX compounds

1.4.1 Bond order

In MAX phase, the crystal structure and bond order affect the properties. Assuming the case of Al containing MAX phases, the values of bond order for M-X bonds is highest, indicating their greater stability and are then followed by M-A bonding. The bond order values for M-M and A-A bonding are relatively small, showing they are relatively less stable than the former. The M-M bonding not only includes the bond formed between two M atoms of the same layer but also the bonds which are formed between two M atoms belonging to two different layers, which are separated by either an A layer or an X layer. Further, cohesion of a compound is largely affected by the magnitude of bond order and number of bonds together. Within a single M layer, six bonds are formed between each M atoms and only three bonds are formed between M and nearest A or X atoms. Moreover, M-A or M-X bonds adds to the in-layer cohesion the reason for this is these bonds are not perpendicular to the layer. So, although the bond order number appears to be large for the M-X and M-A bonding than those for intralayer A-A and M-M (intralayer is referred to the bonding between atoms of the same layer) but overall M-X or M-A bonding are not that strong. The large length of M-A bonding makes them weaker in comparison to M-X bonding. Also the M layer next to A layer is stronger than the one which is far. M-A bonding are about 20-40% larger than that of M-X bonding. These weak M-A bonding are the roots for the rise for excellent properties of MAX phases that makes them machinable, resistant to thermal shock and highly damage tolerant [34].

1.4.2 Number of M-C slabs

The properties of MAX phase are affected by number of M-C (n) slabs and they also affect the lattice parameters. There is a linear decrease in the values of lattice parameters-a and c, with increasing VEC of M atom. With increasing n, lattice parameter (a) remains unchanged however c parameter increases. 3d compounds have higher lattice parameter than that of 4d and 5d. With increasing atomic diameter, the lattice parameter also increases linearly. But, this effect becomes weak with increasing n [35].

1.5 Nb-Al-C System

Among all MAX phases synthesized to date, Nb_2AlC displays very diverse set of properties. Among the large group of M_2AX phases it exhibits highest softening temperature and bending strength [36]. It is stable with high values of electrical and thermal conductivities [37]. **Scabarozi *et al***. [38] studied and reported superconductivity for Nb_2AlC at 440 mK. This property is quite unique among the group of M_2AX carbides and nitrides. The resistivity of Nb_2AlC is slightly higher than that of V_2AlC. The resistivity for Nb_2AlC at temperature less than 70 K is 0.29 μΩm. The thermal coefficient of expansion for Nb_2AlC is 8.7×10^{-6} K^{-1} which is close to Ti_2AlC (8.2×10^{-6} K^{-1}) and Ta_2AlC (8.0×10^{-6} K^{-1}). However, it is lower than that of Cr_2AlC (13.3×10^{-6} K^{-1}). The thermal diffusivity at room temperature for Nb_2AlC is 0.08×10^{-4} m^2/s and specific heat capacity is 382.6 $J.(kg.K)^{-1}$ [39]. The thermal conductivities of Nb-containing compounds increase slightly with increasing temperature. The value of thermal conductivity, at room temperature for Cr_2AlC is lowest and V_2AlC has highest with Ti_2AlC and Nb_2AlC lying in between. The thermal conductivity of Nb_2AlC is 22 $W(m\cdot K)^{-1}$, that is smaller in comparison to that of Ti_2AlC and Ta_2AlC [40]. Just like other MAX compounds, Vickers hardness for Nb_2AlC also decreases as the indentation load increase and it reaches a value of 4.5 GPa in load range of 50-300 N. From the literature, it is clear that microstructural stability of Nb_2AlC is notably good. When examined the grain size of hot isostatically pressed samples of Nb_2AlC it came out to be ≤15 μm, which proves that Nb_2AlC is an excellent candidate for the high temperature applications [41]. But, its oxidation resistance ability in air, is need to be improved to a large extend. These reasons are responsible for further study of Nb_2AlC compound.

2 Literature Review

In MAX phase family, Al containing compounds are of specific interest as they form the largest group and this large stable group of Al containing compounds shows great potential for development of self-healing materials. MAX phases with Al and Si are of special interest since the oxides of these A elements have been shown to act successfully as healing agents [42, 43]. Ti_2AlC, being a member of the MAX-Phase ceramics family has shown an unusual ability to heal cracks multiple times through selective oxidation of Al, while maintaining its salient mechanical properties [44]. The literature was surveyed by keeping in mind the various synthesis routes for MAX compounds, so as a part of it synthesis mechanism of following MAX phases was studied:

Synthesis of Ti_2AlC

Ti_2AlC was first synthesized in year 1963, as a thin layer employing the CVD method [45]. Further, in year 1976 by another method [46] in which it was synthesized directly from powder of Ti, Al and lampblack at 900-1000 °C, 1 h under argon atmosphere. The resultant cakes were ground to powders and sintered in vacuum at 1500 °C yielding a 90–92% dense Ti_2AlC. In year 1997, fully dense bulk polycrystalline Ti_2AlC was fabricated by reactive hot pressing (RHP) the combined mixture of Ti, Al_4C_3 and C powders at 1600 °C, 40 MPa, 4 h [47] and after that in year 2000 it was synthesized by reactive hot isostatic pressing (RHIP) at 1300 °C and at same pressure but for 30 h [48]. The material obtained had grain size of at least 20 μm and was relatively soft (5 GPa). But the major drawback of these routes was the necessary requirement of very high temperature furnaces, very long processing periods, large holding times and uneconomical encasing from outer environment.

In year 2002, Ti_2AlC was synthesized by from the Ti-Al-C elemental powder blend. For this purpose **Y. Khoptiar and I. Gotman** [49] employed the thermal explosion mode (TE) of self-propagating high-temperature synthesis (SHS) which is done either in a furnace by applying pressure simultaneously. TE mode was ignited at low temperatures around 670 °C and was preceded by the melting of Al. Combustion synthesis of Ti_2AlC was found to proceed in several stages: (1) Firstly, Ti aluminides were formed by self-sustained reaction between Ti and Al; (2) TiC, TiC_{1-x} were formed which resulted from a self-sustained reaction between Ti and C; (3) Reaction between solid $TiC_{0.6}H_{0.7}$ and liquid Ti aluminides resulted in the evolution of Ti_2AlC. A high degree of conversion (up to 90% Ti_2AlC) was achieved during pressureless thermal explosion; however, the samples obtained were porous. A mild and tolerable pressure

of 30 MPa was applied when reactive forging was done at 800 °C, which resulted in formation of >98% dense Ti_2AlC samples that contained ternary carbide in an appreciable amount of TiC_{1-x}.

All these year's many researchers tried to synthesise MAX phase, in powder and bulk form by using different methods like chemical vapor deposition, solid-state synthesis, self-propagating high temperature synthesis, annealing, hot isostatic pressing, pulse discharge synthesis and deposition of MAX phase as thin film was also achieved by magnetron sputtering. Spark plasma sintering (SPS) has been proved successful in synthesizing all the refractory ceramics. Its advantages over hot pressing had led to its wide area application. Some of its properties includes faster densification, small sintering periods and low sintering temperature.

In 2004, spark plasma sintering (SPS) of Ti, Al and C powders in molar ratio of 2:1.2:1 at 1100 °C, 30 MPa for 1 h, synthesized polycrystalline Ti_2AlC. Examined density of the synthesized sample was 99.8% of the theoretical value. **Mei *et al.*** [50] optimized the ideal synthesis temperature of Ti_2AlC which came out to be 1100 °C. This temperature was the lowest temperature for fabricating high purity Ti_2AlC. The grain size of the as synthesized Ti_2AlC was about 20 µm long and about 5 µm in thickness. Its Vickers hardness came out to be 4 GPa.

The Al-containing MAX phase have attracted the most attention, some of them, such as Ti_2AlC and Ti_3AlC_2 [51] have unusual oxidation resistance which arises from the formation of a thin alumina layer at their surface. They also endure extraordinary self-healing properties, wherein the formed cracks are filled with alumina. Among all the MAX phases synthesized till date, aluminium containing MAX compounds is large in number. For Al containing MAX phases, M-X bonds have highest bond order showing that they are more stable, followed by M-A bonds and then M-M and A-A bonds.

Synthesis of Cr_2AlC

Cr_2AlC, one of the members of MAX phase's group was introduced for the first time in the year 1963 by **Jeitschko** [52]. In spite of its unusual properties Cr_2AlC did not gain much popularity because its bulk synthesise is inflexible and vigorous. In year, 1980 **Schuster *et al.*** [53] synthesized it by sintering Cr, Al and C powder through arc melting. The sealed samples were annealed at 600 °C and 1200 °C (170–500 h) and lastly its quenching was done in water. But due to its low productivity this method was only limited to laboratory fabrication.

Theoretical calculation of Cr_2AlC and a series of M_2AX phases done by **Sun *et al***. [54] and **Lofland *et al.*** [55], led to the result that revealed that among few Al containing MAX phases

(specifically M_2AlC, M = Ti, V, Cr, Nb and Ta) Cr_2AlC had the highest theoretical bulk modulus which resulted from the fact that in Cr_2AlC, M–C bond energy is largest. Further review of mechanical properties of Cr_2AlC revealed it had properties equivalent to that of Ti_3SiC_2 [56].

Lin *et al.* [57] in year 2005, had successfully produced single phase bulk Cr_2AlC by solid-liquid (S-L) reaction. Sintering of powder samples of Cr, Al and C was done at 1400 °C and 1350 °C for 60 min and 30 min, respectively. In year, 2006, Reactive HIPing of Cr, Al and graphite powder resulted single-phase, fully dense, polycrystalline samples of Cr_2AlC. But, the method employed by **Manoun *et al.*** [58] was very complex.

So in year 2007, **Tian *et al.*** [59] attempted to synthesise Cr_2AlC by employing molten salt method. Cr (average size around 3μm), Al, graphite powders, NaCl and KCl were taken as initial ingredients. According to the stoichiometric ratios the composition was taken as Cr:Al:C = 2:1:1 and 2:1.1:1. The different content of powder and salt were taken in ratio as 1:2, 1:1 and 2:1. The mixture was then wet ball milled in alcohol using Si_3N_4 for 24 h. The mixture was then dried and packed in vacuum quartz tube. The tubes were then heated at different temperatures of 900-1200 °C with holding time of 1 h. The powders so obtained was sintered and then washed with de-ionized water and then dried. The obtained powders were subjected to hot pressing at 1400 °C for 1 h under 20 MPa.

In 2009, **Zhou *et al.*** [60] employed hot pressing to fabricate Cr_2AlC. Cr, Cr_3C_2 and Al powders were the starting materials. The resultant product was subjected to phase determination by XRD and microstructure was studied by SEM. The Cr_2AlC were seen to possess columnar and plate like grains.

Further in year 2014, **Arbab** [61] chose molten salt method for synthesis of Cr_2A1C powders. To synthesize Cr_2A1C bulk piece with high density, the powders were sintered. The results showed that the most purity of Cr_2AlC powder can be achieved when raw materials ratio was 2Cr/2A1/C and powder to salt ratio is 1:2 heated at 1100 °C for 1 h. The density of bulk piece had been calculated about 90% of the theoretical density. The hardness was measured to be 5 GPa and modulus values came out 204 GPa.

Synthesis of Ti_3SiC_2

Ti_3SiC_2 has better thermal and electrical conductivity than Ti metal, despite of its excellent mechanical properties, it is easily machinable. Although, it was first synthesized and its structure was determined in 1960 [62], however, its potential as a useful high temperature material was not possible because of the difficulty of fabricating single-phase, bulk polycrystalline samples. Though some work to synthesize by chemical vapor deposition [63, 64] was done but due gaseous reaction its small scale fabrication was restrained.

In the 1960s, Hans Nowotny's group in Vienna pulled discovered more than 100 new carbides and nitrides [5]. But until 1990, these phases remained unexplored and in mid-1990s MAX phases gained popularity, when in year 1996 **Barsoum** and **El-Raghy** [65] successfully fabricated Ti_3SiC_2 by hot isostatic pressing (HIPing), which is more attractive powder based process than conventional CVD. Pure samples of Ti_3SiC_2 was synthesised by mixing**,** powder Ti, C, and SiC in ratio of 3:1:2 respectively and were cold pressed at 180 MPa and then hot pressed at 1600 ºC for 4h under a pressure of 40 MPa. The XRD indicated presence of single phase Ti_3SiC_2. However, the back scattered SEM micrographs revealed the almost 2 vol% SiC in TiC_x in the final sample. The sample was again subjected to HIPing at 1600º C and Ti_3SiC_2 pure sample was obtained. Its compressive strength, at room temperature was measured to be 600 MPa but it dropped to 260 MPa at 1300 °C in air. The room temperature conductivity was measured as 4.5×10^6 $(\Omega m)^{-1}$, which is twice that of pure Ti. The thermal expansion coefficient in temperature range 25 °C to 1000 °C, room temperature thermal conductivity and the heat capacity are 10×10^{-6} $°C^{-1}$, 43 W/(m.K) and 588 J/(kg.K) respectively. But their synthesis process was characteristic of the relatively coarse SiC powder, with a diameter of 99 µm.

Li *et al.* [66] in year 1999, synthesised Ti_3SiC_2 by using Ti (16 µm >99.6% purity), Si (70 µm >99.9% purity) and C (5 µm >99.7% purity). The powder mixture was prepared in three ways: hand mixing for 30 min using mortar and pestle, wet ball milling in ethanol solution for 100 h, dry ball milling for 500 h in argon atmosphere. In ball milling, they used a jar and balls made up of Si_3N_4 in which the slurry obtained from wet ball milling were vacuum dried and pulverized. The mixed powder was formed into billets by die pressing and subsequent cold-isostatic pressing. The green compact so obtained was then fired with in a BN crubical in argon atmosphere at 0.1 MPa. The obtained sample was examined by X ray diffraction technique. Dense Ti_3SiC_2 sample was prepared by reactive hot pressing. The green compact was first coated with BN powder to a thickness of 1mm and then inserted into borosilicate glass tube; the coating of BN prevented any reaction between the green compact and the glass. The tube

was then evacuated and heated to the softening temperature of glass (780 ºC). Then, sealed and burn with a glass flame cutter, the encapsulated specimen was then hot isostatically pressed in argon atmosphere. The obtained powder was heat treated at low pressure and temperature was then increased with holding time of 2 h.

In year 2002, **Li *et al.***, [67] synthesised Ti_3SiC_2 powder by mechanical alloying (MA) in which the elemental powder of Ti, Si, and C were used. The MA conditions were studied and the effect of ball size was studied. The fabrication conditions were strongly affected by ball size. Use of large balls (20.6 in diameter) helped in formation of Ti_3SiC_2 which may be due to triggering of a combustion reaction from the effect of balls on the powder. On the other hand, it was concluded that the synthesis of Ti_3SiC_2 phase could not be achieved by using small balls (12.7 mm in diameter). The mechanical alloyed powder was then annealed resulting in fine powders containing 95.8 vol% of Ti_3SiC_2. Since there is more probability of Ti reacting with C, so Ti_3SiC_2 could not be obtained by MA process alone. However, milling of the elemental powders to a fine state and then heat treating them at low temperature produced product with high Ti_3SiC_2 concentration.

Zhu and **Mei** [68] in year 2003, synthesized Ti_3SiC_2 by SPS. The elemental powders of Ti, Si, Al, and graphite powders were taken as starting materials to fabricate Ti_3SiC_2. The mixture was first mixed in ethanol for 24 h, after filling it into the graphite dye, it was sintered. Heating rate was 80 °C/min, under the vacuum of 0.4 Pa and pressure of 30 MPa. SEM micrographs showed that Ti_3SiC_2 fabricated was in plane-shape with a size of about 10–20 μm in the elongated dimension. It was studied that there was decrement in the thermal stability of Ti_3SiC_2 for solid solution of Al and also decreased the decomposition temperature of Ti_3SiC_2 to 1300 °C.

Synthesis of Nb_2AlC and Nb_4AlC_3

Fabrication of MAX based materials, however, is mainly based on hot-pressing technique. An external pressure is required to accelerate solid state reaction between the powder components. Thus, only simple shape components can be produced which limits the freedom of shaping as well as the manufacture of products. **Hu *et al.*** [69], in year 2008, successfully synthesized Nb_4AlC_3. Powder of Nb, aluminium and graphite were mixed in molar ratio was taken to be Nb:Al:C= 4.1:3:2.7. Excess aluminium was used, because aluminium could be lost at high temperatures, while processing, powders were mixed in resin jar and ball milled for 24 h and then uniaxially pressed at 5 MPa to form a green compact in BN graphite die which was then

heated at 1500 ºC, 1000 ºC, 1650 ºC and 1700 ºC under flowing Ar atmosphere, at heating rate of 15 ºC/min. The sample was then held at a target temperature for 60 min under a pressure of 5 MPa. Its thermal conductivity increased from 13.5 to 21.2 $W\cdot(m\cdot K)^{-1}$ but there was decrement in the value of electrical conductivity, which went down from 3.35×10^6 to 1.13×10^6 $(\Omega m)^{-1}$. Its flexural strength and high temperature toughness is 346 MPa and 7.1 $MPa\cdot m^{1/2}$ respectively. The high temperature properties of Nb_4AlC_3 are noteworthy, its flexural strength retains at very high temperature of 1400 °C and its Young's modulus retain up to 1580 °C, which in comparison to Nb_2AlC (1400 °C), β-Ta_4AlC_3 (1200 °C), and Ta_2AlC (1200 °C) is very high.

In year 2009, **Zhang *et al.*** [70], synthesized Nb_2AlC by using powders of NbC, Nb and Al was mixed in molar ratio 1:1:1. The mixture was then wet ball milled using acetone as a dispersant for 24 h, using Al_2O_3 balls 5 mm in diameter. After the acetone was evaporated, the mixture was pressed at 5 MPa to form green compact graphite die. The powder was divided into two sets, one set was heated in hot press in flowing Ar atmosphere upto 600, 700, 900, 1100, 1300, 1500 and 1650 ºC with a heating rate of 15 ºC/min. Samples were held at that temperature for 30 min at a pressure of 1 MPa and were then cooled down to room temperature. Other set was hot pressed at 1650 ºC by applying pressure of 30 MPa for 90 min. The disks so obtained by hot pressing were cut into rectangular bars, for further characterization. Single phase Nb_2AlC was prepared by reactive hot pressing at 1650 °C.

In year 2009, Nb_2AlC thin film was synthesized in ultra-high vacuum magnetron sputtering chamber. For this purpose **Scabarozi *et al.*** [71] employed three magnetron cathodes with 2 inch elemental targets and were kept about ∼7 cm above the substrate. The pressure was 5×10^{-8} Torr for each deposition at deposition temperature. Radio- frequency sputtering was carried out in Ar atmosphere maintaining a pressure of 4-18 mTorr. X ray diffraction was done to study the formed phases using Cu-Kα radiation. For micrograph analysis transmission electron microscope (TEM) operating at 200 kV was put to use. TEM micrographs lead to study of interfaces and microstructure.

Textured Nb_4AlC_3 ceramic was successfully fabricated in year 2011 by **Hu *et al.*** [72], using a strong magnetic field accompanied by spark plasma sintering. Nb_4AlC_3 samples were synthesized using Nb, Al, and carbon black as initial materials. Nb_4AlC_3 powder was fabricated as: the bulk Nb_4AlC_3 sample was broken in air and sieved. The powder so obtained was wet ball milled in ethanol, for 24 h using a Si_3N_4 jar in a planetary mill at the rate of 300 rpm. The as-obtained powder was dried and analysed by measuring particle size in the sample, sample

morphology and its composition. It was then textured in a 12 T magnetic field and was then cold isostatically pressed. The green density of the sample was obtained to be 50.4% and 58.7% respectively.

Nb_4AlC_3 retains its strength upto 1400 ºC but it shows poor behaviour at room temperature. Particulate strengthening is a great alternate method to considerably upgrade the weak mechanical properties of MAX phase. For example the properties of Ti_3AlC_2, Ti_3SiC_2 can be improved by incorporating TiC, SiC, TiB and Al_2O_3. So to raise some of the mechanical properties of Nb_4AlC_3, in year 2012, **Zheng *et al.*** [73], used $Nb_5(Si,Al)_3$ to strengthen Nb_4AlC_3 by varying contents of Nb_5 $(Si,Al)_3$(0, 5, 10, 15 20 vol%). Powders of Nb, Si and graphite were used as initial materials which were wet ball milled in ethanol in an agate jar, with agate balls for 24 h. The mixture was then subjected to hot pressing in a graphite mould at 1900 ºC for 1 h, in flowing Ar atmosphere, under the pressure of 30 MPa. The flexural strength of Nb_4AlC_3-15 vol% $Nb_5(Si, Al)_3$ was measured to be 387 MPa at 1400 ºC which is about 89.6% of that of room temperature but it is higher than room temperature flexural strength of monolithic Nb_4AlC_3 (370 MPa).

Applications of Nb_4AlC_3 are limited in number reason being, its poor behaviour against oxidation at high temperature. In year 2013, **Zheng *et al***. [74], tried to improve the oxidation properties by silicon pack cementation. For which, phase pure Nb_4AlC_3 was fabricated by *in situ* hot pressing. Nb, Al and graphite were wet ball milled in ethanol using agate balls and agate jars. The mixture was then subjected to a heat treatment graphite mould for 1 h at 1900 ºC, in flowing Ar atmosphere in 30 MPa. For oxidation test and Si pack cementing, specimen with dimension 10 mm×10mm×2mm were cut from synthesised materials using electric discharge method. The surface was ground with SiC paper then polished and at last cleaned with ethanol. In order to achieve the strengthened Nb_4AlC_2 silicon pack cementation was carried out at 1200 ºC for 6 h. The pack powder consisting of 16wt% Si, 4 wt% NaF and 80 wt% of Al_2O_3, where Si powder fulfilled the necessity of Si source, NaF acted as an active agent and Al_2O_3 as a filling agent. The Si pack cemented Nb_4AlC_3 showed excellent oxidation resistance upto 1200 ºC as the protective Al_2O_3 layer is formed.

Synthesis of $(Cr,Mn)_2GaC$

From 1996 to 2004, intensive research expanded the MAX phase family to more than 60 compositions that included 9 different "M" elements, 12 different "A" elements and n values of 1, 2, and 3. Since then, new discoveries reported have mainly focused on MAX phases with higher n values and on solid solutions by substituting the M, A or X elements, hence giving rise to enormous possible combinations. In 2014, **Naguib *et al.*** [51], listed 60+ already reported quaternary phases. These phases provide the chances of adding those elements that do not form a bulk ternary MAX phase. For example Mn was incorporated in $(Cr_{1-x}Mn_x)_2GaC$ $(0 \leq x \leq 0.3)$ by **Mockute *et al***. [75], in year 2014. Many $(Cr,Mn)_2AlC$ samples were synthesized by varying the molar ratios Cr:Mn:Al:C as 2:0:1.3:1, 1.8:0.2:1.3:1, 1.6:0.4:1.3:1, 1.2:0.8:1.3:1, 0.8:1.2:1.3:1, and 0.4:1.6:1.3:1. The blend of Cr, Mn, Al and graphite powders was cold pressed (at 400 MPa) and then heat treated upto 1400 °C under Ar flow for 1 h. Further in order to obtain a fully dense $(Cr,Mn)_2AlC$, the powders of Cr and Mn were taken in ratio of 1.8:0.2. It was then heat treated to 1400 °C under 39 MPa for 3 h. as the melting point of Ga was low so it was not able to get mixed with the other remaining elements, therefore a different route was used. The starting powder blend of Cr, Mn and graphite were taken in a alumina crucibles and Ga pallets were kept on above so that when Ga melts it reacts with other elements. These were then heated in a glass tube to 975 °C and this temperature was hold for 24 h. in total five samples of $(Cr,Mn)_2GaC$ were synthesized with Cr: Mn: Ga: C molar ratios of 2:0:1:1, 1.5:0.5:1:1, 1:1:1:1, 0.5:1.5:1:1 and 0:1:1:1. All the phase were determined using X-ray diffraction technique. The results revealed that the solubility of Mn in Cr_2AlC and Cr_2GaC, corresponds to the compositions which are $(Cr_{0.94}Mn_{0.06})_2AlC$ and $(Cr_{0.7}Mn_{0.3})_2GaC$. In was studied that in latter sample only one-third of the M-lattice sites were occupied by Mn atoms.

Synthesis of $Zr_2(Al_{0.5}Bi_{0.5})C$

In year 2016, **Horlait *et al.*** [76], synthesized first ever Bismuth containing MAX phase. Zirconium dihydride, bismuth, aluminium and graphite were used as reactants. All the oxygen impurities were prevented by weighing the reactants in Nylon milling jars in an Argon glove box. The 10 mm ZrO_2 balls were used to mill powder for 30 min at 350 rpm. The as milled powder was then sealed to initiate synthesis reaction. The ratio of the powders according to the stoichiometry was examined and confirmed to 2:1.05:0.95 for Zr, Al + Bi and C respectively. Reaction was ignited by giving the heat treatment, in absence of pressure. The powder samples were contained in graphite crucibles, which were given heat treatment in a furnace under Ar atmosphere. Three different synthesis temperatures were tested: 1450 °C (1 h holding time),

1300 °C (10 h holding time) and at 1150 °C (10 h holding time). The heating and cooling rates were ~20 °C. min^{-1}. The powder of $Zr_2(Al_{0.5}Bi_{0.5})C$ obtained after 1300 °C was ground in an agate mortar and underwent a <250 μm sieving to be used for SPS sintering at 1300 °C for 10 minutes. XRD determined that the attempt to synthesize $Zr_2 (Al_{0.50}Bi_{0.50})C$ at 1300 °C was partially successful as a MAX phase was formed along with ZrC and $ZrAl_2$.

From the above literature it was visualized that Nb-Al-C Max phase was not synthesized directly by ball milling. In this work, attempt was made to see the feasibility of their synthesis. Moreover, this will also open a new path for the synthesis of MAX phase.

3 Experimental Work

In this presented work, attempt has been made to synthesize Nb_2AlC MAX phase via ball mill using niobium pentaoxide Nb_2O_5 (*Sigma-Aldrich, 99% purity*) as niobium source, pure aluminium powder (*SDFC Ltd, 99% purity*), activated charcoal (*SDFC Ltd.,*) as carbon source and magnesium (*Lobachemie, 99% purity*) metal powder as reducing agent. For the synthesis of Nb_2AlC various parameters such as amount of reducing agent and milling durations are enlisted in table 3.1 and methodology is being discussed as follows;

Table 3.1: Synthesis conditions for the preparation of Nb_2AlC.

SAMPLE ID's	**AMOUNT OF POWDERS USED (gm)**				**MILLING TIME (hours)**
	Niobium (Nb_2O_5)	**Aluminium (Al)**	**Act. Charcoal**	**Magnesium (Mg)**	
S1-NL	13.29	2	2	2	10
S2-NL	13.29	2	2	2	20
S1	13.29	2	2	2	10
S2	13.29	2	2	2	20
S3	13.29	2	2	2	50
S4	13.29	2	2	2	75
S5	13.29	2	2	5	20

3.1 Methodology

The synthesis of Nb_2AlC was practised using planetary ball mill, since the aim was to synthesise MAX phase in a single step process. The Nb_2O_5 powder, Al powder, activated charcoal powder and Mg powder were mixed all together in molar ratio of 2:1:1: x (where x is amount of magnesium 2 and 5 gm). All the powders were ball milled for different durations using a tungsten carbide jar and tungsten balls of 7 mm diameter in a Retsch Planetary Ball Mill (PM 100). In the balls to powder ration of 10:1, the samples were milled for 10, 20, 50 and 75 h at 300 rpm. The magnesium content was also varied in one of the sample to study its effect. After milling the samples were leached for 12 h in solution of HCL and distilled water in ratio of 1:1. Thereafter, solution was washed several times with distilled water until pH 7

was obtained. It was then dried in oven at 120 °C and then ground using agate mortar and pestle.

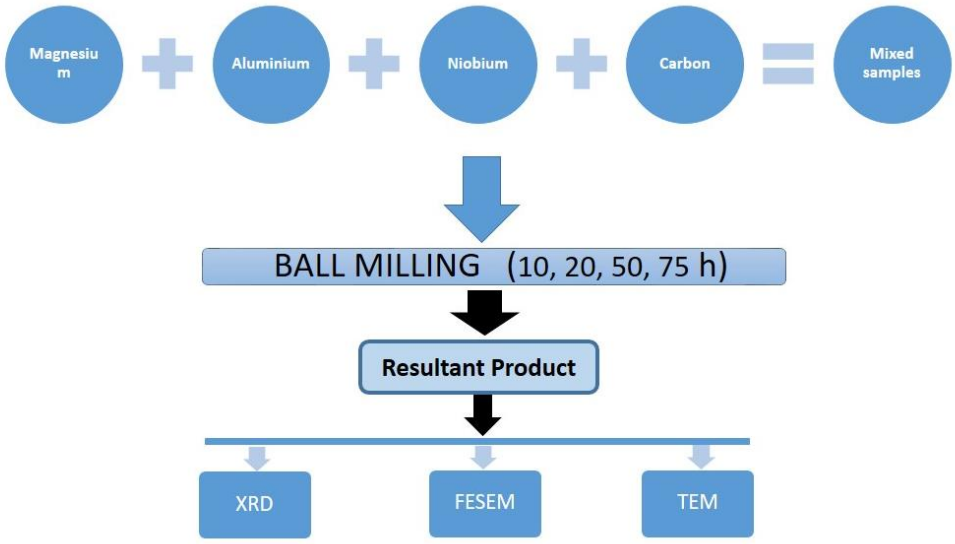

Figure 3.1: Methodology used to synthesize and characterize powder sample.

3.2 Characterization

3.2.1 X-ray diffraction

X-ray diffraction (XRD) is non-destructive analysis technique which provides means to identify different phases and their distribution in the samples. It also helps to analyse texture, average grain size, internal stress of a sample etc. X-rays are electromagnetic waves with wavelength (λ= 0.5-50 Å), comparable to atomic separation distances. When propagating through a crystal, the X-rays interact with the lattice and are diffracted according to the Bragg's law which is as follows;

$$2d \sin\theta = n\lambda$$

where, d is the interplanar spacing, θ is the diffraction angle, n is order of diffraction, and λ is the wavelength of X ray. As the combination of constituent atoms, crystal structure, and lattice constants is different for different phases, XRD provides with a unique set of diffraction angles and diffracted beam intensities, which makes phase identification possible. Since each crystalline solid has its unique characteristic X-ray powder diffraction pattern which may be used for its identification. Bruker Kappa APEX-II was used for this purpose with Cu Kα λ= 1.54060 Å over the range of 15-80° with step size of 0.0190° and XRD analysis was done in *PANalytical X'pert high score* software.

3.2.2 Field Emission Scanning Electron Microscopy (FESEM)

In order to get the topographical information about a material FESEM is used. Both information about topography and elemental knowledge is provided in the magnification range of 10-300,000 X, with virtually unlimited depth of field. The working principle is such that it specifically focuses an electron beam on the specimen. It combines high resolution imaging with analytical functioning. The electrons from the beam produce secondary electrons of low energy that provides topographic information of the specimen. Unlike optical microscope, it uses electrons instead of light and the resolution of optical microscope is limited. Field emission scanning electron microscopy (FESEM) was used to get topographical of the sample for which Nova Nano (FESEM FEI 450) was used at 18 kV.

3.2.3 Transmission Electron Microscope (TEM)

Transmission electron microscopy (TEM) is an invaluable analysis technique for materials investigation at nanoscale. The working principle of TEM is very similar to a conventional optical microscope, though with electrons used instead of visible light. The electrons emitted from a light source are focused with the help of electromagnetic lenses into a very thin and precise beam. When the electron beam enters a specimen, the electrons that travelled to the bottom of the specimen, which are unscattered, they strike the screen which results in shadow image of the material. In this shadow image various parts are visible depending upon the density. These images are captured by a camera for further analysis. The resolution of a TEM is about 0.2 nm and magnification is up to about 10^7X. To observe powder particles using TEM, the powder was dispersed homogeneously in ethanol by sonication, before fogging them onto the Cu grid of 300 mesh size. JEOL 2100 was used to observe TEM micrographs of synthesized samples at accelerating voltage of 200 kV at different magnifications.

4 Result and Discussion

In the proposed work, attempts were made to synthesize Nb_2AlC MAX phase using a single step ball milling process. The different stages of transformation, growth of microstructure and the completeness of the reaction, were determined by X-ray diffraction (XRD), scanning electron microscopy (SEM) and transmission electron microscopy (TEM). The effect of milling time and amount of reducing agent (Mg) was studied which govern the overall reaction during milling.

1.1 X-ray diffraction analysis

The XRD results revealed the different phases formed in the samples. The results were studied by comparing with various standard ICDD cards with the *X'pert Highscore Plus* tool. All the synthesized samples contained NbC as major phase and oxides of niobium, magnesium and aluminium as minor phases. The standard cards from which XRD pattern was matched are enlisted as follows:

Table 4.1: List of ICDD Card used for phase determination

S. No.	ICDD card	Phase	Crystal Structure
1	03-065-7993	NbC	FCC
2	01-089-2120	Nb_4C_3	Cubic
3	00-042-1125	NbO	FCC
4	01-076-1095	NbO_2	Tetragonal
5	01-074-0298	Nb_2O_5	Monoclinic
6	00-004-0787	Al	Cubic
7	01-071-1684	Al_2O_3	Rhombohedral
8	00-001-1148	Mg	Hexagonal
9	00-004-0829	MgO	Cubic

1.1.1 Effect of milling Time

The effect of milling duration for 10, 20, 45 and 75 h on the synthesized powder is shown in figure 4. There are five major diffraction peaks observed for NbC phase for the planes (111), (200), (220), (311) and (222) in every milled sample. These peaks confirm the rock-salt (NaCl) structure of NbC with space group Fm-3m. When Nb_2O_5 and Mg are concurrently present in one system, Mg reduces Nb_2O_5 in a self-sustaining manner to yield elemental niobium and with

it a significant amount of heat is also released. This heat increases the jar temperature which initiates the reaction between niobium and carbon yielding NbC [77]. From figure 4.1 (sample S1), it is clear that Nb_2O_5 is present as a secondary phase in the system which was used as reactant. Its presence depicted the unavailability of milling time for complete reduction of Nb_2O_5. The aluminium supported magnesium to reduce Nb_2O_5 and formed Al_2O_3. When milling time was increased to 20 h (sample S2), it was observed that the broadening of the diffraction peaks of Nb_2O_5, Al_2O_3 and NbO_2 occurred with increasing milling time because there is considerable reduction in crystallite size and subsequent increase in deformation parameter for the reactant powder particles with reduced intensity of minor phases indicating enhanced formation of Nb_4C_3. While in sample S3, Nb_2O_5 content has been reduced due to its reduction and transformation of Nb_4C_3 into NbC was observed. Further, prolonged milling of 75 h (sample S4) resulted single phase NbC accompanied by very small peaks of NbO and Al. As an effect of milling time, lesser duration leads to form carbon deficient niobium crystal lattice (Nb_4C_3) which was converted to NbC at longer milling. No peaks of the MAX phase was observed in any of the XRD patterns which may be due to the fact that the higher affinity of Nb and Al towards oxygen and C as compared to intermediate stage i.e. combination of Nb, Al and C (MAX phase).

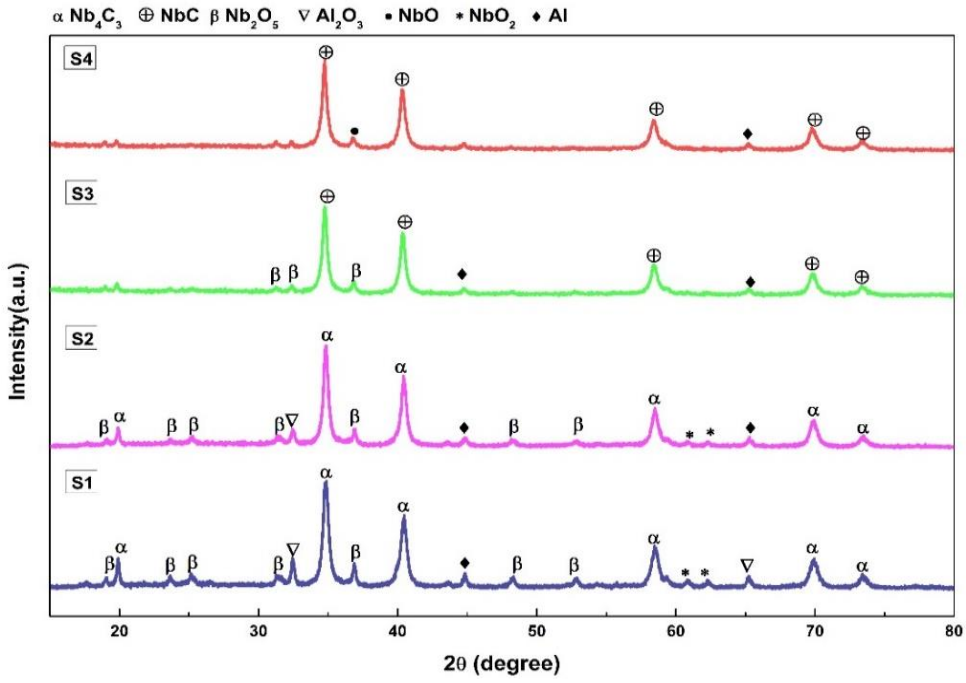

Figure 4.1: Effect of milling time on the synthesis of MAX phase showing intermediate phases.

1.1.2 Effect of amount of reducing agent (Mg)

The effect of reducing agent was also studied by varying the amount of reducing agent 2 g and 5 g. Basically, amount of reducing agent in reactant mixture is directly proportional to the extent of reduction of Nb_2O_5. Such reducing effect is very much clear from XRD pattern of sample S2 and S5 in figure 4.2. Higher Mg content in sample S5 which was milled for 20 h resulted almost complete conversion of Nb_2O_5 to NbC with a very small NbO content. While, lesser amount of Mg (2 g) resulted the mixture of Nb_4C_3, oxides of Nb (Nb_2O_5 and NbO_2), alumina and aluminium metal. With the help such behaviour, it can also be suggested that Mg content also helps the carburization of Nb by reducing the carbon deficiency in lattice i.e. conversion of Nb_4C_3 to NbC.

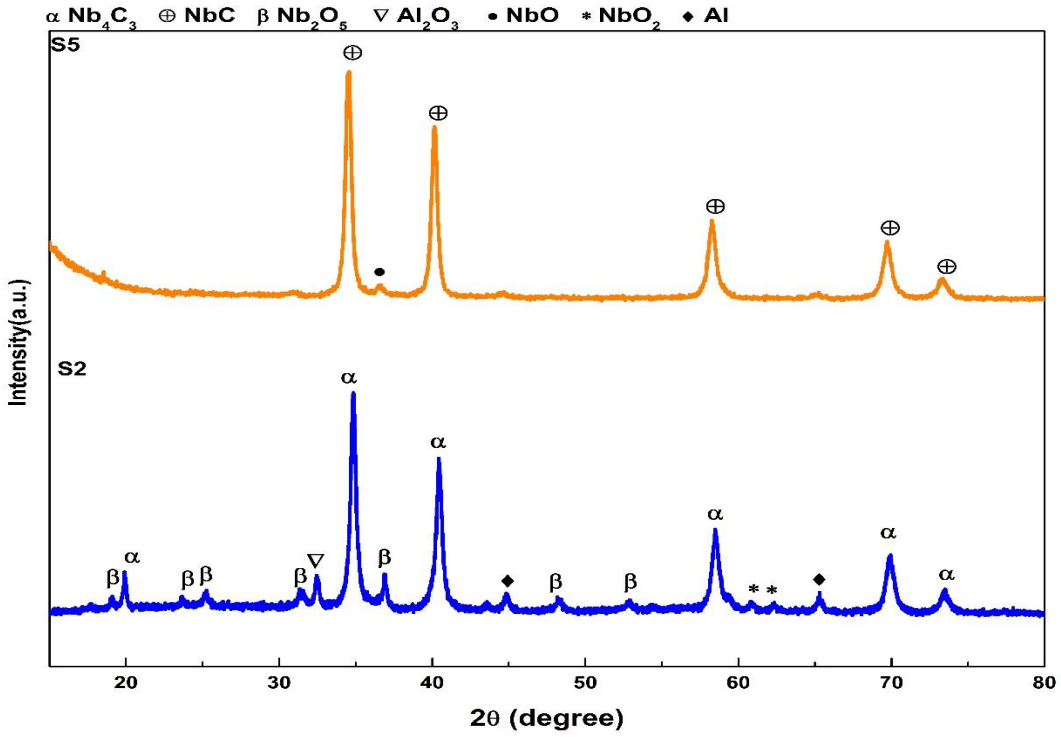

Figure 4.2: Shows the XRD pattern of two samples highlighting effect of magnesium content.

1.1.3 Effect of Leaching

As synthesized powder samples were leached with HCL and distilled water (1:1) solution for 12 h. It is clear that leaching in acidic medium resulted to the removal of Mg and MgO. Effect of leaching on the sample S1 and S2 is shown in figure 4.3. Both the sample contained Mg and MgO in milled sample (sample S1-NL and S2-NL) which has successfully removed from the sample by leaching as shown in figure 4.3. Mg and MgO were converted to $MgCl_2$ which is soluble in water and further removed by washing several time by distilled water [78].

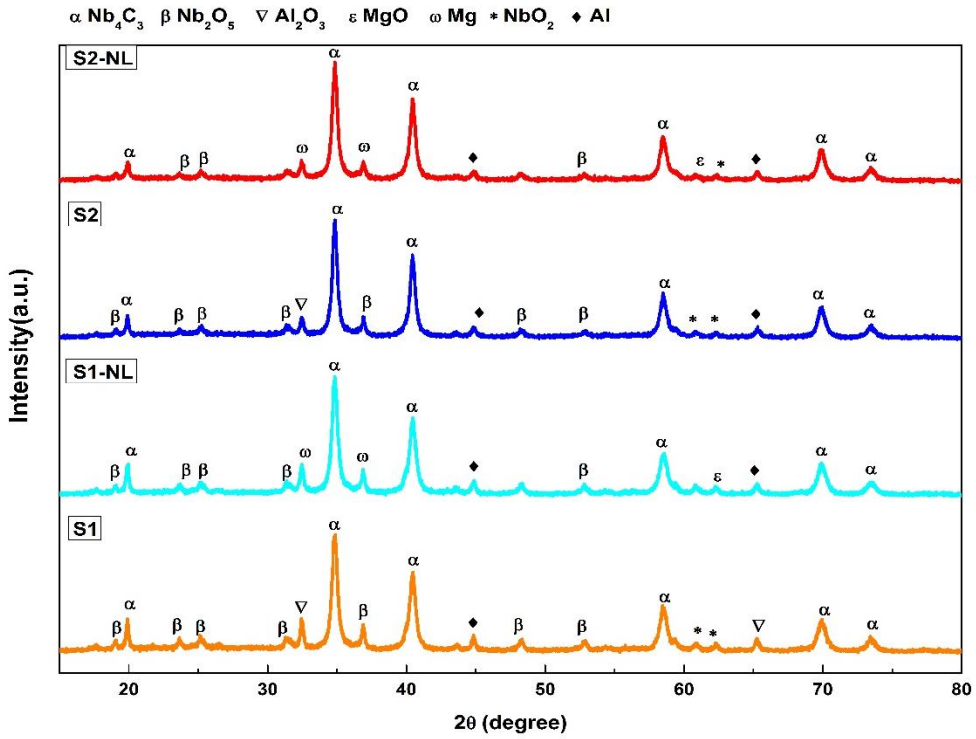

Figure 4.3: Effect of leaching on the synthesized nanopowder.

1.2 Microstructure Analysis

1.2.1 FE-SEM Analysis

For microstructural analysis, samples with least impurities of niobium oxides (Nb_2O_5, NbO and NbO_2) were chosen to observe the morphological features. Figure 4.4 and 4.5 depict the morphological microstructures of samples S4 and S5 respectively. Both the samples have huge layered agglomerates of nanoparticles which may be due to the shear action on reduced particle size of sample during ball milling as shown in figure 4.4 and 4.5 After 75 h of milling (sample S4, figure 4.4), large agglomerates consisting of very fine particles were observed. During ball milling, both the welding and micro forging processes occurred in the initial stage of milling. Besides welding, the process of fracturing within the powder particles also occurred during collisions between the balls and powder particles. The high temperature of the process leads to the formation of dense agglomerates. Therefore, the powders became agglomerated layers with extremely low thickness and facilitated solid state reaction to occur [79, 80].

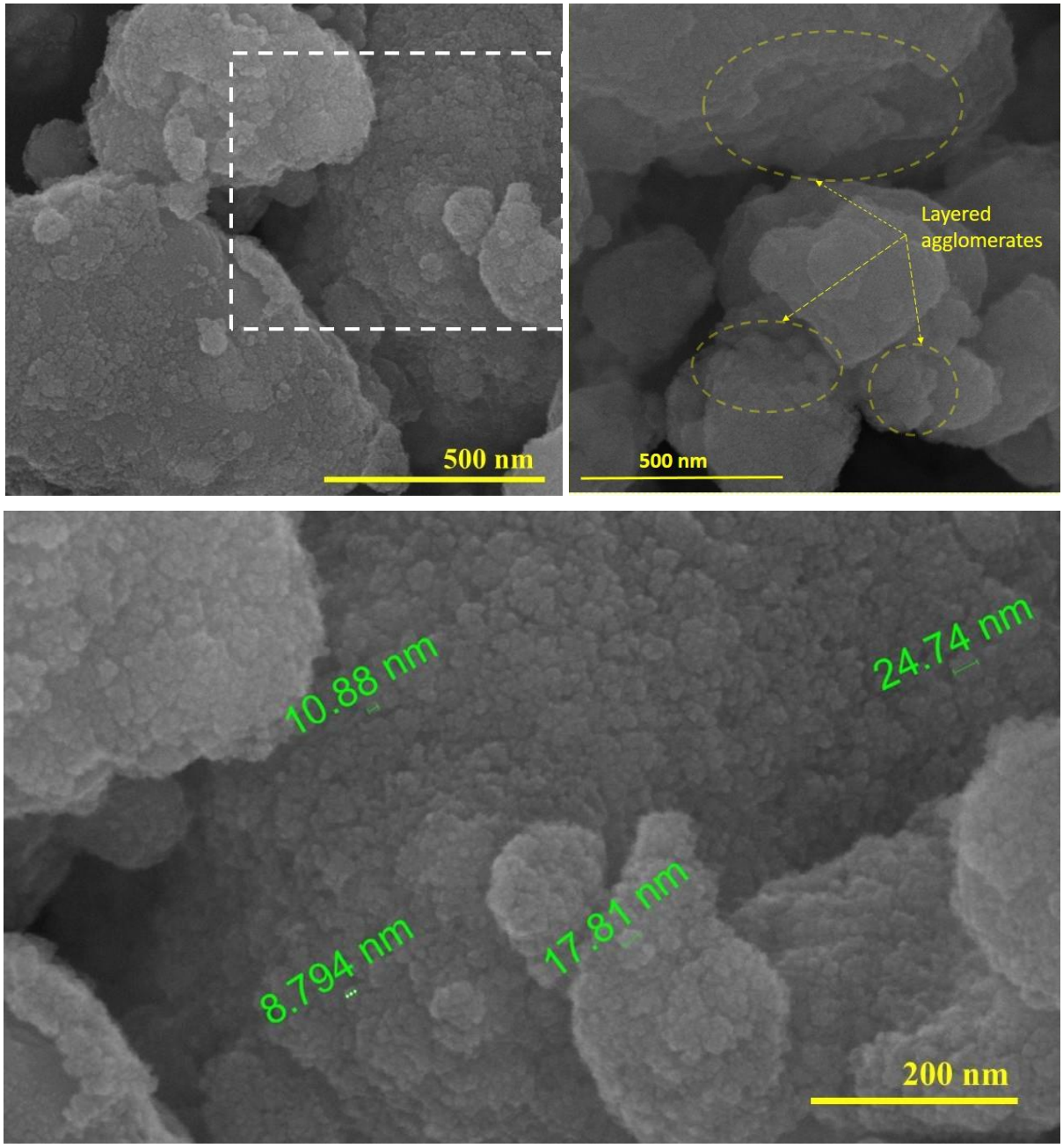

Figure 4.4: FESEM of sample S4 (which is milled for 75 h with 2 g magnesium) having huge agglomerates of nanoparticles.

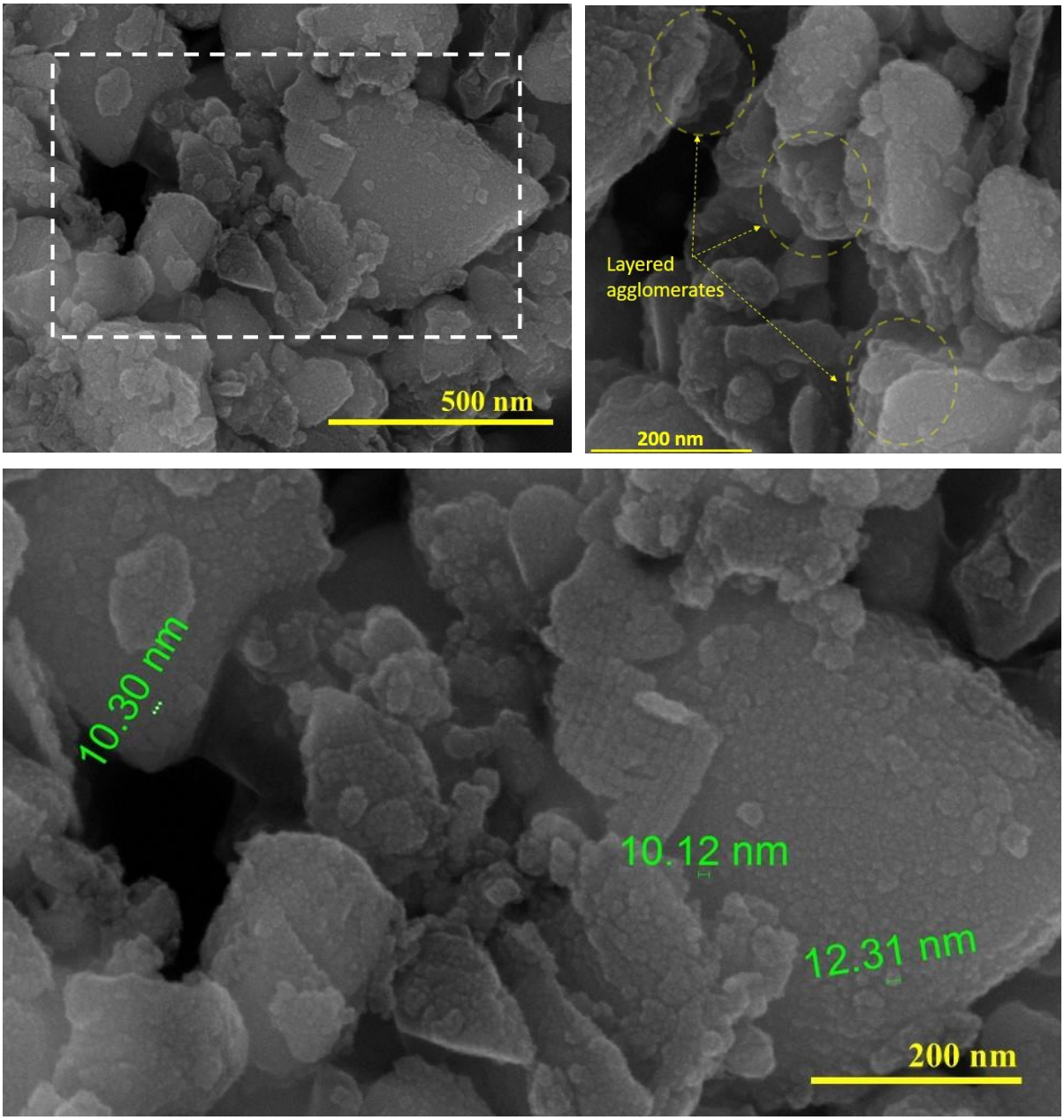

Figure 4.5: FESEM image of sample S5 milled for 20 h with 5 g magnesium.

1.2.2 Particle Size Distribution

The particle size is measured with the help of AxioVi-sion Rel.4.9.1.0 for both the samples and it came out to be 10.14 nm for S4 and 6.76 nm for S5. Since there is precise particle size distribution so it is beneficial to plot the frequency of particles against the logarithm size of the particle. The particle size follows the following lognormal distribution function:

$$\mathbf{f\,(d)} = \frac{1}{\sqrt{2\pi}.\ \sigma.\mathrm{di}}\, e^{-\left(\frac{(\log(di)-\mu)^2}{2\sigma^2}\right)}\mathbf{;\ where}\quad \mu = \frac{\log\sum(di)}{\sum ni}\quad \mathbf{and}\quad \sigma = \sqrt{\frac{\sum(\log(di)-\mu)^2}{\sum ni}}$$

Where f (d) designates the lognormal distribution of particle size, di represents the size of ith particle of NbC, Σni is the total number of particles in consideration, μ is mean diameter and σ is the standard deviation of particle size.

Sample S4 possessed steeper nanoparticle's size distribution as compared to sample S5 which may be associated to the higher reduction rate of Nb_2O_5 due to the higher Mg content in the reactant mixture. Higher reduction rate of Nb_2O_5 triggers the reaction early and more nucleation sites were provided to the formation of NbC which is supported by the figure 4.6 having smaller probability with smaller particle size i.e. ~6.9 nm for sample S5.

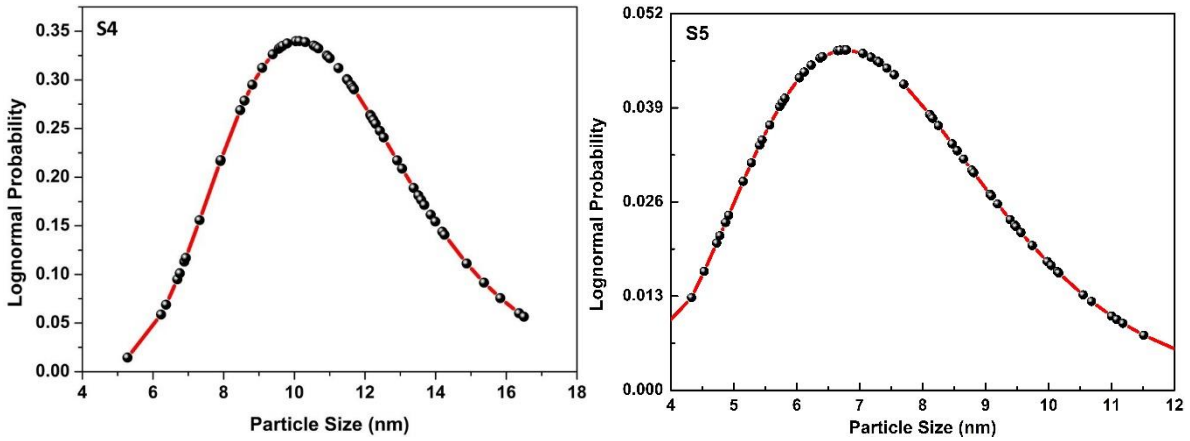

Figure 4.6: Lognormal particle size distribution of the sample S4 and S5.

1.2.3 Transmission Electron Microscopy (TEM) Analysis

Figure 4.8 and 4.9 show the TEM micrographs of sample S4 and S5 suggesting the high degree of agglomeration of nano particles respectively. Micrographs show the features as a function of contrast of the picture. The dark portions in figure 4.8 and 4.9 render the agglomerated layers of the nanoparticles (as shown in figure 4.4 and 4.5) comprising of a thin layer on each agglomerate. Figure 4.8 and 4.10 show the selected area electron diffraction (SAED) pattern of sample S4 and S5 respectively, which is uniform with high crystallinity of the samples. The diffraction rings from inner to outer side correspond to (111), (200), (222) and (331) planes of NbC respectively. The presence of diffraction spots suggests the nano crystallinity of the prepare samples. High resolution TEM micrograph of S5 suggests the nanocomposite nature of prepared sample with the presence of Al_2O_3 and NbC which is shown in figure 4.10 (a).

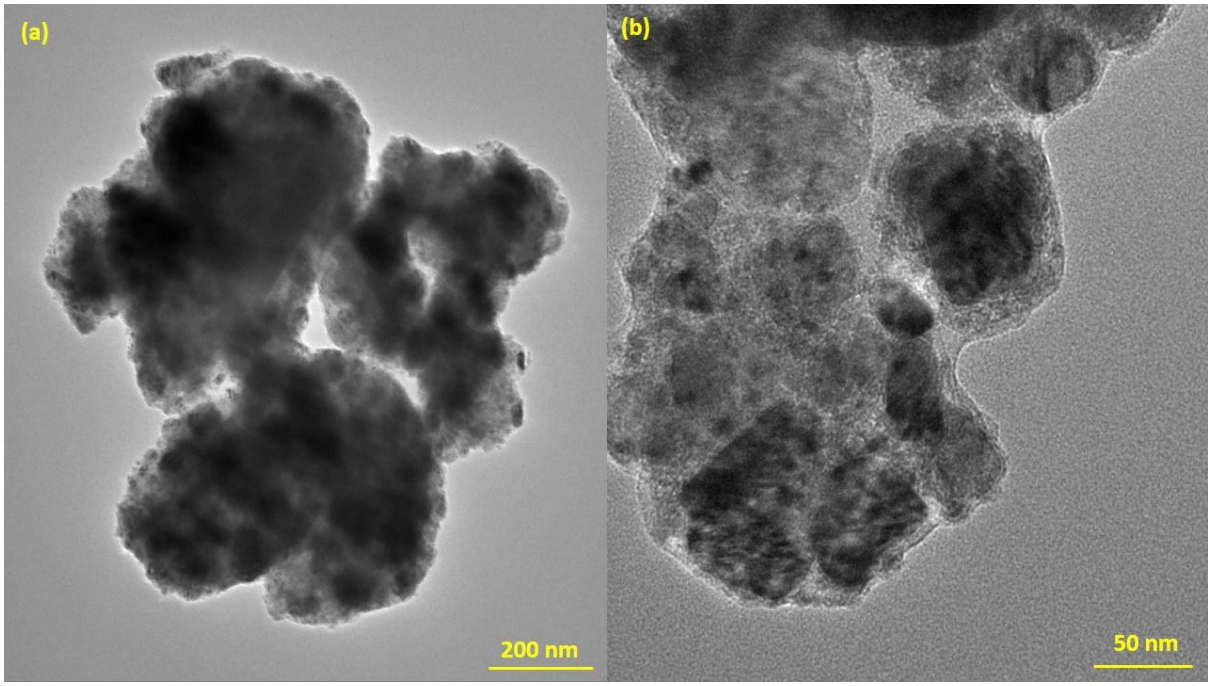

Figure 4.7: HR-TEM micrographs of sample S4 showing very large agglomerates of nanoparticles.

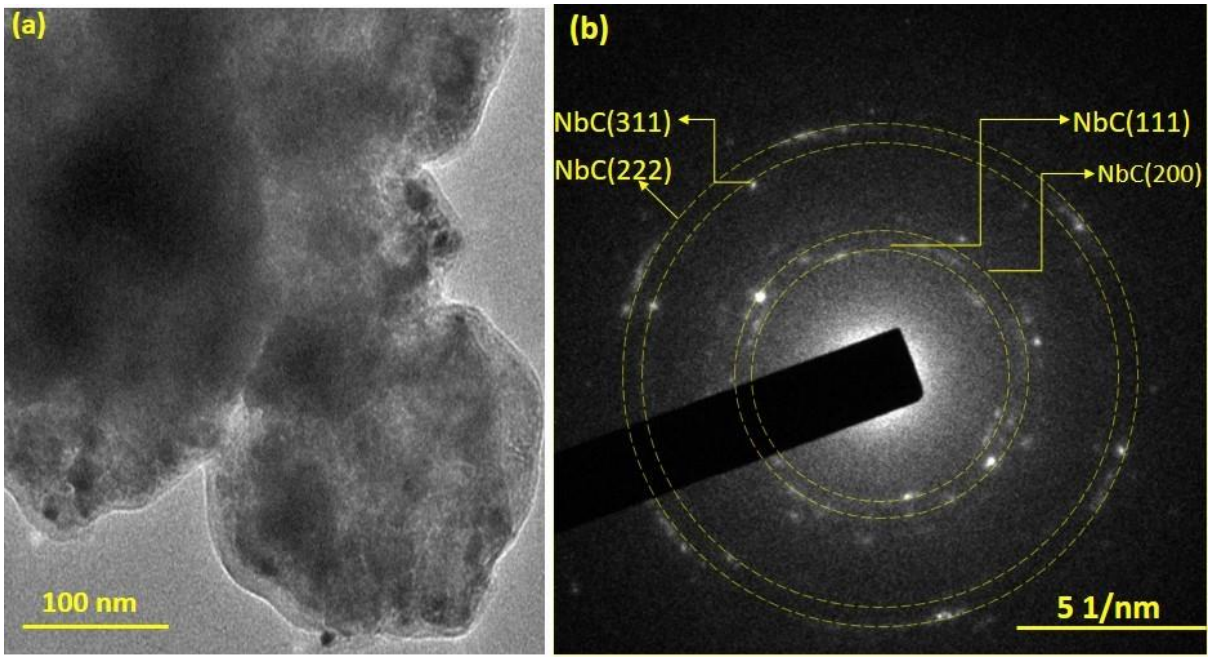

Figure 4.8: SAED pattern of the sample S4 depicting the presence of NbC.

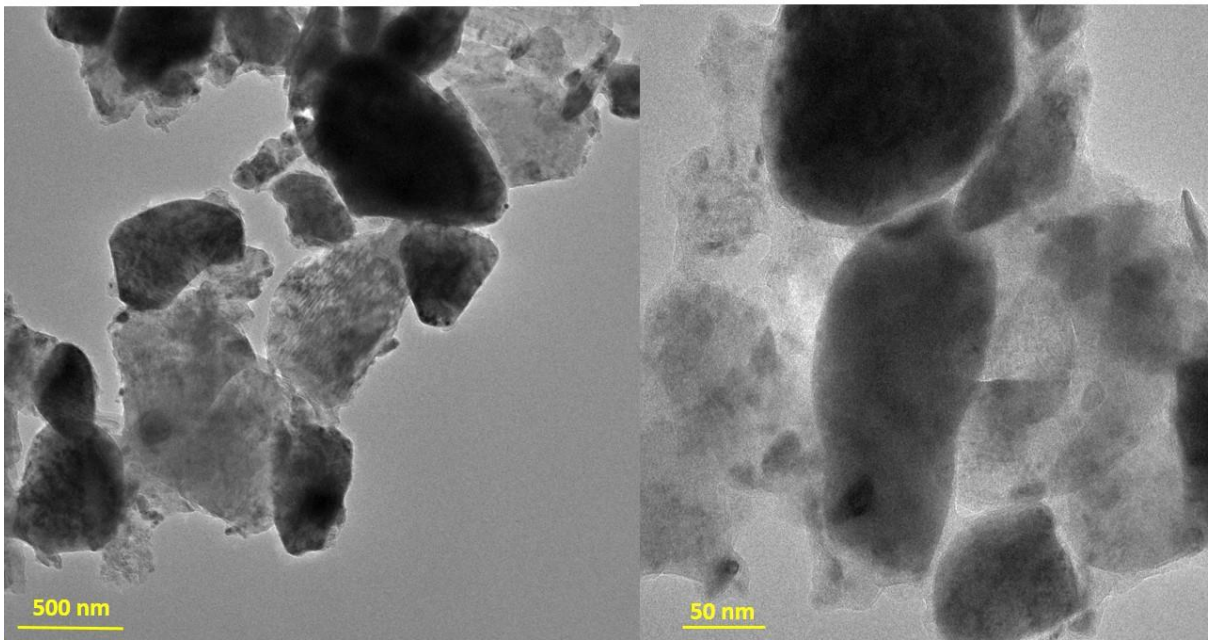

Figure 4.9: HR-TEM micrographs of the sample S5 suggesting faceted morphology of agglomerates.

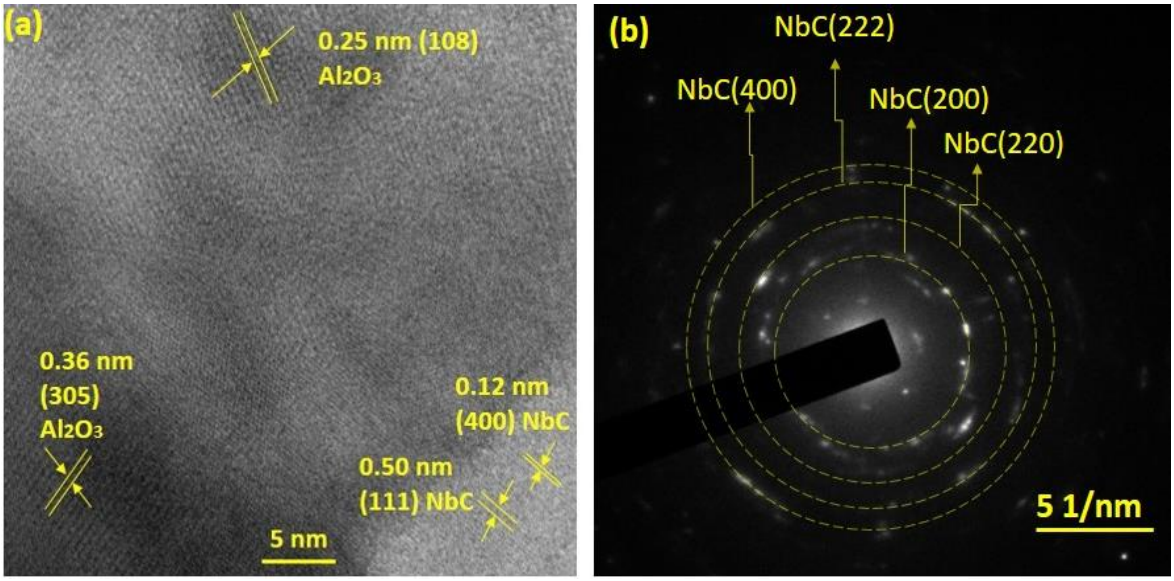

Figure 4.10: HR-TEM image of sample S5. (a) HR-TEM micrograph of sample S5 indicating that the powder is nanocomposite of Al_2O_3 and NbC. (b) SAED pattern suggesting the presence of NbC.

5 Conclusion and Future Scope

In summary, Nb_2AlC was not successfully synthesised by only ball milling. From the XRD pattern it is evident that for all the five synthesized samples, no peak of MAX phase was found. Milling time and amount of reducing agent were the parameters that were optimized to obtain MAX phase. Starting results of XRD revealed that amount of reducing agent needed to be increased as peaks of Nb_2O_5 were clearly visible. Increasing the amount of reducing agent helped in reduction of Nb_2O_5 considerably but that enhanced growth of NbC phase rather that MAX phase. The resultant product is a nanocomposite comprising of niobium carbide and Al_2O_3 which is synthesised at room temperature by ball milling.

Future scope

Other technical parameters like balls to powder ration (BPR) and rotation per minutes (RPM) could be optimised. Concentration of aluminium is another parameter that need to be optimised as aluminium evaporates and is easily lost at low temperatures. The literature survey indicates that ball milling followed by sintering can be used as secondary technique to ensure the phase growth.

6 References

1. W. D. Callister, Materials Science and Engineering, John Wiley & Sons, 2007.
2. E. K. Storms, The Refractory Metal Carbides, Academic Press, New York, 1967.
3. H. O. Pierson, Handbook of Refractory carbides and nitrides, Noyes Publications, U.S.A, 1996.
4. M. I. Baraton, Material Science of Carbide, Nitride and Boride, Springer Netherlands, 1999.
5. H. Nowotny, Prog. Solid State Chem., 5 (1971) 27.
6. M. Radovic and M. W. Barsoum, American Ceramic Society Bulletin, 92 (2013) 20.
7. A. Guitton, A. Joulain, L. Thilly and C. Tromas, Scientific Reports, 4 (2014) 1.
8. C. Shih, R. Meisner, W. Porter, Y. Katoh, and S. J. Zinkle, Fusion Reactor Material Program, 55 (2013) 78.
9. Md. A. Rahman, Md. Z. Rahaman, American Journal of Modern Physics, 4 (2015) 75.
10. P. Eklund, M. Beckers, U. Jansson, H. Hogberg and L. Hultman, 8 (2010) 1851.
11. M. W. Barsoum and M. Radovic, Annual Review of Materials Research, 41 (2011) 195.
12. N. I. Medvedeva, D. L. Novikov, A. L. Ivanovsky, M. V. Kuznetsov, A. J. Freeman, Physical Review B, 58 (1998) 16042.
13. M. W. Barsoum, MAX Phases: Properties of Machinable Ternary Carbides and Nitrides, Wiley-VCH, 2013.
14. Aurelija Mockute Synthesis and Characterization of New MAX Phase Alloys (Doctoral Dissertation), Linkoping University, (2014), Dissertation No. 1573.
15. P. Finkel, M. W. Barsoum, T. El-Raghy, J. Appl. Phys., 87 (2000) 1701.
16. P. Finkel, B. Seaman, K. Harrell, J. D. Hettinger, S. E. Lofland, A. Ganguly, M. W. Barsoum, Z. Sun, S. Li, and R. Ahuja, Phys. Rev. B, 70 (2004) 085104.
17. S. E. Lofland, J. D. Hettinger, K. Harrell, P. Finkel, S. Gupta, M.W. Barsoum, G. Hug, Appl. Phys. Lett. 84 (2004) 508.
18. N. Haddad, E. G. Caurel, L. Hultman, M. W. Barsoum, and G. Hug, J. Appl. Phys., 104 (2008) 023531.

19. R. S. Kumar, S. Rekhi, A. L. Cornelius, M. W. Barsoum, Appl. Phys. Lett., 86 (2005) 111904.

20. B. Manoun, R. P. Gulve, S. K. Saxena, S. Gupta, M. W. Barsoum, and C. S. Zha. Phys. Rev. B, 73 (2006) 024110.

21. M. W. Barsoum, H. I. Yoo, I. K. Polushina, V. Yu. Rud, Yu. V. Rud, and T. El-Raghy, Physical Review B, 62 (2000) 10194.

22. M. W. Barsoum, T. Zhen, S. R. Kalidindi, M. Radovic & A. Murugaiah, Nature Materials, 2 (2003) 107.

23. M. Khazaei, M. Arai, T. Sasaki, M. Estili, and Y. Sakka, J Phy. Cond. Matt., 26 (2014) 505503.

24. K. M. Gupta, Engineering Materials: Research Applications and Advances, CRC Press, Taylor & Francis Group, London, 2015.

25. J. D. Hettinger, S. E. Lofland, P. Finkel, T. Meehan, J. Palma, K. Harrell, S. Gupta, A. Ganguly, T. El-Raghy, and M. W. Barsoum, Physical Review B, 72 (2005) 11520.

26. Y. Bai, X. He, R. Wang, and C. Zhu, Journal Of Applied Physics, 114 (2013) 173709.

27. L. E. Toth, Journal of Less Common Metals, 13 (1967) 129.

28. K. Sakamaki, H. Wada, H. Nozaki, Y. Onuki, and M. Kawai, Solid State Communications, 112 (1999) 323.

29. D. Bortolozo, O. H. Sant'Anna, M. S. da Luz, C. A. M. dos Santos, A. S. Pereira, K. S. Trentin, and A. J. S. Machado, Solid State Communications, 139 (2006) 57.

30. S. E. Lofland, J. D. Hettinger, T. Meehan, A. Bryan, P. Finkel, S. Gupta, M. W. Barsoum, and G. Hug, Physical Review B, 74 (2006) 174501.

31. D. Bortolozo, O. H. Sant'Anna, C. A. M. dos Santos, and A. J. S. Machado, Solid State Communication, 144 (2007) 419.

32. D. Bortolozo, Z. Fisk, O. H. Sant'Anna, C. A. M. dos Santos, and A. J. S. Machado, Physica C: Superconductivity, 469 (2009) 256.

33. R. Shein and A. L. Ivanovskii, Physica Status Solidi B, (2011), VOL. 248, pp 228.

34. M. W. Barsoum, Prog. Solid State Chem., 28 (2000) 201.

35. Y. Bai, X. He, R. Wang, S. Wang and F. Kong, Computational Materials Science, 91 (2014) 28.

36. C. F. Hu, F. Z. Li, L. F. He, M. Y. Liu, J. Zhang, J. M. Wang, Y. W. Bao, J. Y. Wang, Y. C. Zhou, Journal Of The American Ceramic Society, 91 (2008) 2258.

37. M. W. Barsoum, I. Salama, T. El-Raghy, J. Golczewski W. D. Porter, H. Wang, H. J. Seifert, F. Aldinger, Metallurgical and Materials Transactions A, 33 (2002) 2775.

38. M. W. Barsoum, I. Salama, T. El-Raghy, J. Golczewski W. D. Porter, H. Wang, H. J. Seifert, F. Aldinger, Thin Solid Films, 517 (2009) 2920.

39. C. F. Hu, L. F. He, J. Zhang, Y. W. Bao, J. Y. Wang, M. S. Li, and Y. C. Zhou, J. Eur. Ceram. Soc., 28 (2008) 1679.

40. M. W. Barsoum, I. Salama, T. El-Raghy, J. Golczewski, W. D. Porter, H. Wang, H. J. Seifert, and F. Aldinger, Metall. Mater. Trans. A, 33 (2002) 2775.

41. I. Salama, T. El-Raghy and M. W. Barsoum, Journal of Alloys and compounds, 347 (2002) 271.

42. H. J. Yang, Y. T. Pei, J. C. Rao, J. T. Hosson, S. B. Li, G. M. Song, Scripta Materialia, 65 (2011) 135.

43. T. Osada, W. Nakao, K. Takahashi, K. Ando, S. Saito, Journal of the European Ceramic Society, 27 (2007) 3261.

44. S. Li, G. Song, C. Kwakernaak, W. G. Sloof, Journal of the European Ceramic Society, 32 (2012) 1813.

45. W. Jeitschko, H. Nowotny, F. Benesovsky, Monatsch. Chem., 94 (1963) 672.

46. W. Jeitschko, H. Nowotny, F. Benesovsky, Mona V. I. Ivchenko, M. I. Lesnaya, V. F. Nemchenko, T. Ya. Kosolapova, Porosk. Metall., 161 (1976) 45.

47. M. W. Barsoum, T. El-Raghy, J. Mater. Synth. Process., 5 (1997) 197.

48. M.W. Barsoum, M. Ali, T. El-Raghy, Metall. Mater. Trans., 31A (2000) 1857.

49. Y. Khoptiar, I. Gotman, Materials Letters., 57 (2000) 72.

50. B. Mei, W. Zhou, J. Zhu and X. Hong, Journal Of Material Science, 39 (2004) 1471.

51. M. Naguiba, G. W. Bentzela, J. Shaha, J. Halimab, E. N. Caspic, J. Lub, L. Hultmanb and M. W. Barsoum., Mater. Res. Lett., 2 (2014) 233.

52. W. Jeitschko, H. Nowotny, F. Benesovsky, Montash. fur Chemie, 94 (1963) 672.

53. J. C. Schuster, H. Nowotny, C. Vaccaro, Journal of Solid State Chemistry, 32 (1980) 137.

54. Z. M. Sun, S. Li, R. Ahuja, Schneider, Solid State Commun., 129 (2004) 589.

55. S. E. Lofland, J. D. Hettinger, K. Harrell, P. Finkel, S. Gupta, M. W. Barsoum, G. Hug, Appl. Phys. Lett., 84 (2004) 508.

56. W. B. Tian, P. L. Wang, G. J. Zhang, Y. M. Kan, Y. X. Li, J. Am. Ceram. Soc., 90 (2007) 1663.

57. Z. J. Lin, Y. C. Zhou, M. S. Li, J. Y. Wang, Z. Metall., 96 (2005) 291.

58. B. Manoun, R. P. Gulve, S. K. Saxena, S. Gupta, M. W. Barsoum, and C. S. Zha Phys. Rev. B, 73 (2006) 024110.

59. W. B. Tian, P. L. Wang, Y. M. Kana, G. J. Zhang, Y. X. Li, D. S. Yan, Mater. Sci. Eng. A., 443 (2007) 229.

60. W. B Zhou, B. C. Mei , J. Q. Zhu, Material Science, 27 (2009) 973.

61. F. Arbab, Int. J. Rev. Life. Sci., 4 (2014) 37.

62. W. Jeitschko and H. Nowotny, Monatsh. Chem., 98 (1967) 329.

63. J. Nickl and K. K. Schweitzer, J. Less-Common Metals., 263 (1972) 35.

64. T. Goto and T. Hirai, Mater. Res. Bull., 22 (1987) 1195.

65. M. W. Barsoum and T. El-Raughy, Journal of the American ceramic society, 79 (1996) 1953.

66. J. F. Li, F. Sato, R. Watanabe, Journals of material science letters, 18 (1999) 1595.

67. J. F. Li, T. Matsuki, R. Watanabe, 85 (2002) 1004.

68. Z. Jiaoqun and M. Bingchu, Journal of Material Synthesis and Processing, 10 (2003) 353.

69. C. Hu, F. Li, L. He, M. Liu, J. Zhang, J. Wang, Y. Bao,J. Wang, Y Zhou, Journal of The American Ceramic Society, 91 (2008) 2258.

70. W. Zhang, N. Travitzky, C. Hu, Y. Zhou, P. Greil, Journal of The American Ceramic Society, 92 (2009) 2396.

71. T. H. Scabarozi, J. Roche, A. Rosenfeld, S.H. Lim, L. Salamanca-Riba, G. Yong, I. Takeuchi, Thin Solid Films, 517 (2009) 2920.

72. C. Hu, Y. Sakka, H. Tanaka, T. Nishimura, S. Grasso, Journal of the American Society, 94 (2011) 410.

73. L.Y. Zheng, J. Y. Wang, J. X. Chen, M. Y. Liu, Y. J. Sun, Y. C. Zhou, journal of The American Society, 96 (2012) 365.

74. L. Zheng, J. Wang, Y. Zhou, Journal of The American Ceramic Society, 97 (2013) 552.

75. A. Mockute, J. Lu, E. J. Moon, M. Yan, B. Anasori, S. J. May, M. W. Barsoum & J. Rosen, Materials Research Letters, 3 (2015) 16.

76. D. Horlait, S. C. Middleburgh, A. Chroneos, W. E. Lee, Scientific Reports, 6 (2016) 1.

77. M. Jalaly, M. Sh. Bafghi, M. Tamizifar, F. J. Gotor, Journal of Alloys and Compounds, 588 (2004) 36.

78. H. N. Bae, M. S. Choi, G. G. Lee and S. H. Kim, Materials Transactions, 56 (2015) 1875.

79. J. Eckert, I. Borner, Mat Sci Eng a-Struct, 240 (1997) 619.

80. K. Wolski, G. L. Caer, P. Delcroix, R. Fillit, F. Thevenot, J. LeCoze, Mat Sci Eng a-Struct, 207 (1996) 97.